Available online at www.sciencedirect.com

ScienceDirect

Procedia Engineering 213 (2018) 459–469

Procedia Engineering

www.elsevier.com/locate/procedia

7th International Conference on Fatigue Design, Fatigue Design 2017, 29-30 November 2017, Senlis, France

On the fatigue behavior of notched structural adhesives with considerations of mechanical properties and stress concentration effects

Vinicius Carrillo Beber[a,b]*, Bernhard Schneider[a], Markus Brede[a]

[a] *Fraunhofer IFAM, Wiener Straße 12, Bremen 28359, Germany*
[b] *Universität Bremen, Fachbereich 4, Bibliothekstraße 1, Bremen 28359, Germany*

Abstract

In this work, three types of structural modified epoxy adhesives were used to investigate the effect of stress concentrations on the fatigue behavior of notched bulk specimens. SN curves of un-notched and notched specimens were determined at constant amplitude and R = 0.1 in the range between $N_f = 10^3$ (LCF) and $N_f = 10^6$ (HCF). The following key conclusions were made: (i) fatigue strength was reduced due to the presence of notches, especially at the HCF; (ii) adhesives showed different values of notch sensitivity with values for the adhesives lower than typical values of metals; (iii) for un-notched samples fatigue strength was between 62 and 78% of tensile strength for $N_f = 10^3$ and around 50% for $N_f = 10^6$; (iv) for notched samples fatigue strength was between 67 and 78% of the tensile strength for $N_f = 10^3$ and around 40% for $N_f = 10^6$; (v) fractography evidenced the presence of voids and shear yielding around the notches, (vi) unnotched samples showed the same fracture behavior for both LCF and HCF with crack formation at the external surface. For notched samples there was a significant distinction between LCF and HCF with cracks forming at the notch root.

Peer-review under responsibility of the scientific committee of the 7th International Conference on Fatigue Design.

Keywords: Fatigue; Stress concentration; Adhesives; Notch; Fractography; SN curve; Mechanical properties

* Corresponding author.
E-mail address: vinicius.carrillo.beber@ifam.fraunhofer.de

1877-7058
Peer-review under responsibility of the scientific committee of the 7th International Conference on Fatigue Design.
10.1016/j.proeng.2018.02.045

1. Introduction

Adhesively bonded structures are frequently used under cyclic loading conditions (*e.g.* rotating blades, engine vibration) making them sensitive to fail due to fatigue [1]. The phenomenon of fatigue, which involves the phases of crack nucleation and crack propagation, is very complex [2]. For instance, the presence of stress concentrations, *i.e.* notches, is a known factor that can severely alter the fatigue behavior of structural adhesives due to several reasons [3]:

- formation of a multi-axial state of stress;
- creation of non-uniform stress distribution;
- increase in local strain rate;

These factors combined make it difficult to accurately predict the fatigue lifetime of notched components. For this reason, designers often rely on large safety factors in order to ensure reliability of structural bonded structures against fatigue failure [4]. Since one of the driving forces for the use of structural adhesive bonding is the reduction of weight, part of this benefit is lost due to an over conservative design with subsequent cost and performance consequences [2].

Nomenclature

A1, A2, A3	types of structural adhesives
U	un-notched specimen
N	notched specimen
B	negative inverse slope of SN curve
FSL	fatigue strength loss
N_f	number of cycles to failure
k_F	fatigue notch factor
k_T	stress concentration factor
q	notch sensitivity
R	stress ratio
S_a	nominal stress amplitude
S_H	hydrostatic stress
S_{max}	maximum value of stress during a cyclic loading
S_{min}	minimum value of stress during a cyclic loading
S_o	y-intercept of SN curve
S_{VM}	von Mises stress
T	triaxiality

Since the 50's with the pioneering works of Neuber [5] and Peterson [6] several authors have dealt with the effect of notches on the stress concentrations of materials. In the case of polymeric materials Takano and Nielsen [7] investigated the stress-strain behavior of a wide range of notched polymers. They observed that polymeric materials react differently according to their mechanical properties (*e.g.* ductility). Katnam *et al.* [3] focused their work on a two-part epoxy paste adhesive. They demonstrated the formation of a stress-whitening region around the notches and that failure stress was higher with increasing triaxiality. For the case of fatigue loading, most of the available works on notch effects were focused on polymers. The main observations that can be summarized are: (i) alteration of slope of the SN curve [8,9] and (ii) reduction of fatigue performance with stronger effects at the high cycle fatigue [10–12]. Regarding structural adhesives Beber *et al.* [13] investigated the fatigue behavior of notched bulk specimens of toughened epoxies. They obtained SN curves whilst measuring the damage due to stiffness

degradation. The main conclusions were that the presence of notches reduced fatigue strength and caused damage acceleration.

Structural adhesives can be used for different applications where different mechanical responses are to be expected, for instance, impact absorption or vibration damping. Hence, adhesives are chemically designed to present different mechanical properties with regards to stiffness, ductility, and strength. In this regard a better understanding of the effect of stress concentration on the fatigue behavior of structural adhesives (with different mechanical properties) can support the design of adhesively bonded structures. In order to assess the effect of stress concentrations, a potential approach that had been proved valid is the use notched bulk specimens. This approach presents the advantages of [14,15]: (i) simplicity of production, (ii) mode of testing remains the same for un-notched and notched specimens, and (iii) no effect of the adherend in the results of testing.

In this context, the present work aims to investigate the effect of stress concentration on the fatigue behavior of notched bulk specimens of structural adhesives and correlate findings with their mechanical properties. To achieve this, the following objectives were set:

- to determine SN curves of notched and un-notched specimens;
- to conduct fractography analysis using optical microscopy;
- to perform linear-elastic Finite Element Analysis to support the understanding of results.

2. Structural Adhesives

Three different types of structural adhesives (A1, A2, A3) were used for the current investigation. All three adhesives are hot cure single components (see Table 1) belonging to the so-called class of modified epoxies with the following characteristics: combination of high stiffness from a highly cross-linked epoxy matrix with enhanced toughness due to the addition of secondary particles. The process of sample manufacturing is described in Section 3.1. Representative curves of the stress-strain behavior of adhesives are shown in Fig.1

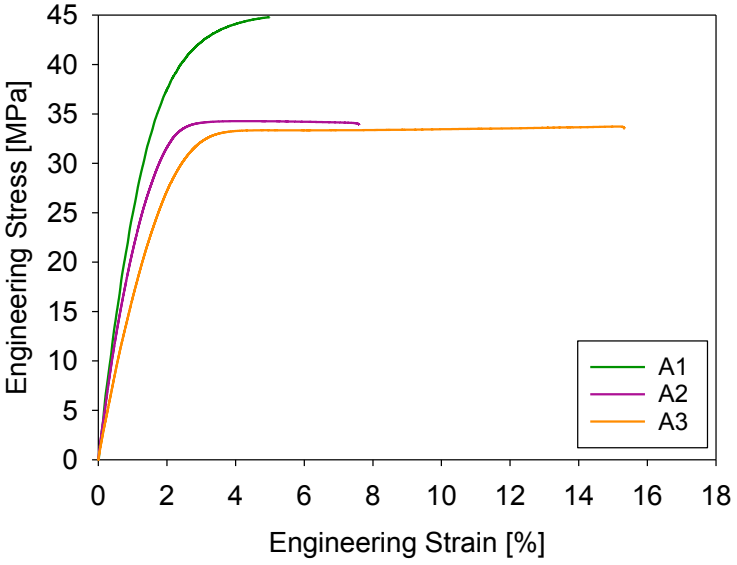

Fig. 1. Representative curves of the stress-strain behavior of the adhesives under investigation

Mechanical properties, mean values, and standard deviation of five experiments under quasi-static testing conditions of un-notched specimens are described in Table 1. The quasi-static tests were conducted under displacement control with a displacement rate of 2mm/min.

Table 1. Mechanical properties and curing conditions of the structural adhesives under investigation

Mechanical property	Adhesive – A1	Adhesive – A2	Adhesive – A3
Tensile strength [MPa]	44.6 ± 0.2	35.1 ± 2.4	34.0 ± 0.2
Young's modulus [MPa]	3050.1 ± 77.6	2298.4 ± 127.4	1761.3 ± 15.6
Tensile strain at break [%]	4.9 ± 0.2	7.3 ± 0.9	16.9 ± 2.8
Poisson's ratio [-]	0.4	0.4	0.4
Curing conditions	175°C / 20 min	175°C / 20 min	180 °C / 30 min

3. Experimental methodology

3.1. Sample manufacturing

Since all adhesives were hot-cure single components, the steps of manufacturing the bulk specimens were the same. The only difference was related to temperature and time of cure, as seen in Table 1. For manufacturing, adhesive cartridges were heated up to 55°C (application temperature) in order to obtain a suitable viscosity for the use of a pneumatic-gun with controlled pressure. The adhesive was applied on plasma treated steel plate with anti-stick properties (Fig. 2a). Spacers were placed between plates to set the desired sample thickness (5 mm). Mechanical properties of bulk adhesives are highly dependent on the temperature, time of curing, and pressure level [16]. For this reason, curing was performed in a hot-press with a load of 10kN.

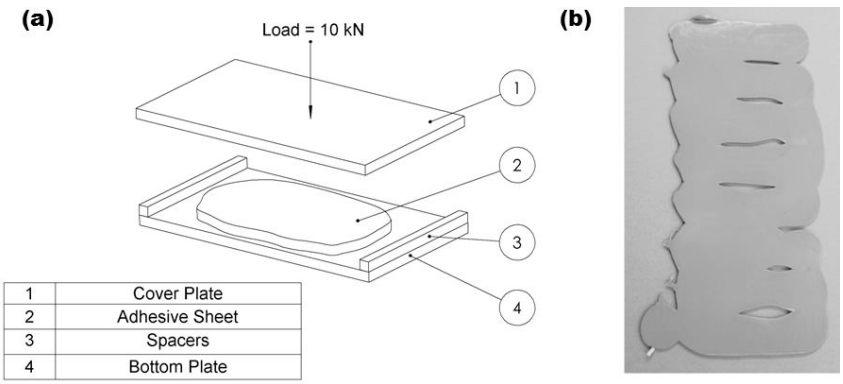

Fig. 2. Manufacturing process of bulk specimen (a) production set-up; (b) adhesive plates

After curing, adhesive sheets (Fig. 2b) were milled according to dimensions shown in Fig. 3.

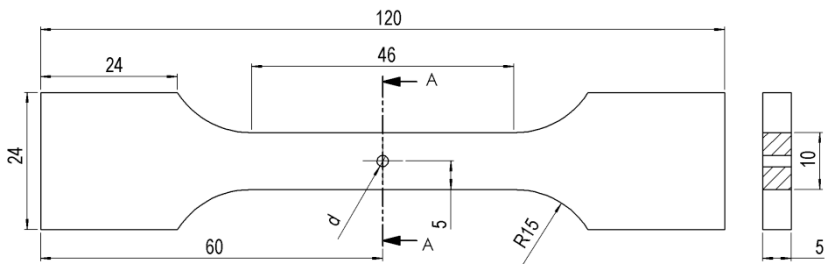

Fig. 3. Dimensions of the bulk specimen with detail of notch (internal drilling)

Finally, in the case of notches specimens, a one millimeter hole was drilled in to the sample.

3.2. Fatigue testing and fractography

Quasi-static and fatigue testing was conducted in an electrodynamic testing machine Instron E3000 with a load capacity of ± 3 kN. Tests were carried out under constant amplitude with force control in a cyclic tension-tension loading with sinusoidal shape, stress ratio ($R= S_{max}/S_{min}$) of = 0.1, and a frequency of 7 Hz. The chosen frequency was determined based on earlier investigation by our research group [13]. This was the highest possible frequency (reduction of testing time) without the risk of thermal heating affecting the results. Stress amplitudes ($S_a= (S_{max}-S_{min})/2$) were defined so as to capture lifetimes in the low to high cycle range ($10^3 < N_f < 2.10^6$).

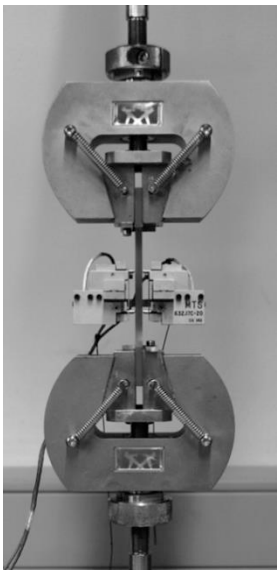

Fig. 4. Quasi-static and fatigue testing set-up

After failure fracture surfaces were analyzed using an optical microscope with CMOS Sensor (Keyence VHX-S50).

4. Finite Element Analysis

To support the understanding of fatigue results FEA was carried out to obtain the normalized maximum principal stress and stress triaxiality distributions of the notched specimen. Normalized maximum principal stress (S_I) was calculated by dividing the values of the maximum principal stress by the net nominal applied stress (force per net initial area, excluding the notch region). Stress triaxiality (T) was calculated with Equation 1 from the distribution of hydrostatic stress (S_H) and von Mises stress (S_{VM}).

$$T = \frac{S_H}{S_{VM}} \tag{1}$$

Simulations were performed with commercial software Dassault Systèmes Abaqus 6.11-1®. A 2D model under plane stress conditions was used in the simulations. Material behavior was considered to be linear-elastic with tensile properties (Young's modulus and Poisson's ratio) taken from Table 1.

Boundary conditions, as seen in Fig. 5, were defined to reproduce tensile loading. To decrease simulation time, a quarter of the model was simulated using symmetry conditions. Additionally, elements of the sample that were clamped to the machine were removed from the model.

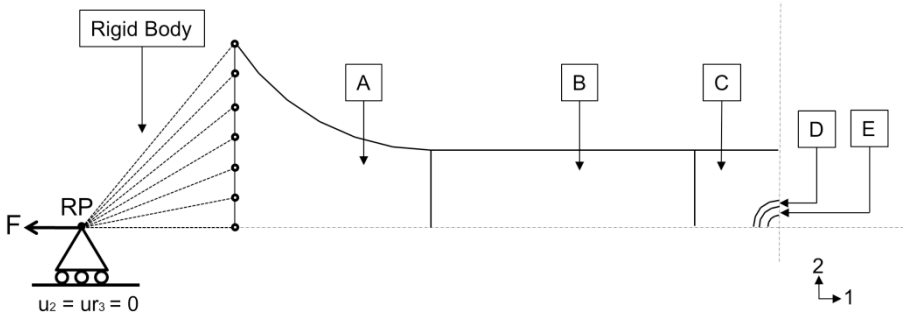

Fig. 5. Boundary conditions of FEA simulation of notched specimen

A reference point (RP) where the force was applied was positioned under sliding conditions in the x-axis. The RP was connected to the model with a rigid body condition. Meshing of the adhesive was carried out using CPS8 (8-node biquadratic plane stress quadrilateral) elements. Mesh was refined according to the distance from the notch root (highest stressed region). Different regions of meshes are labeled A (coarser) to E (finer) in Fig. 5.

Since a linear-elastic analysis was performed and adhesives had the same value of Poisson's ratio, the values of normalized maximum principal stress and stress triaxiality were also the same. There results of FEA simulations are plotted in Fig. 6

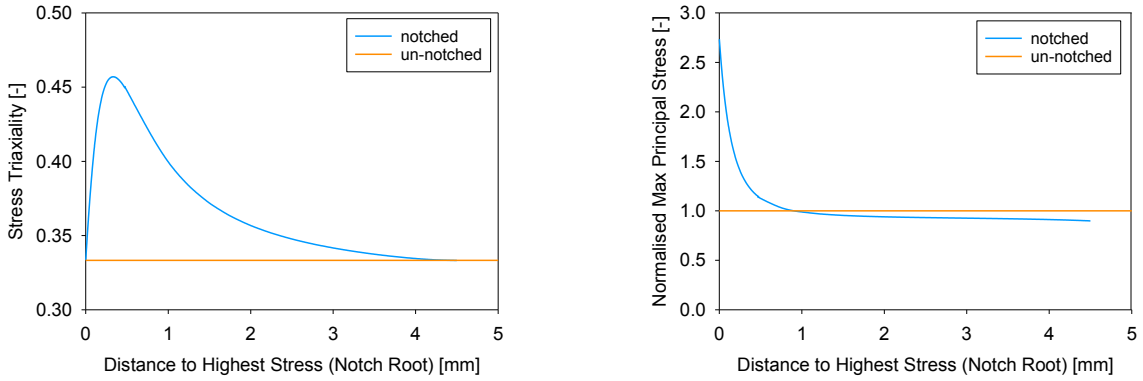

Fig. 6. FEA results - stress triaxiality (left) and normalized maximum principal stress (right)

As expected, a higher value of triaxiality is observed in the region close to the notch root. Moreover, the value of peak stress at the notch root was of $k_T = 2.73$ with a strong stress concentration up to about 1.0 mm away from the notch root. In the next section results of fatigue test will be correlated to stress triaxiality and stress distributions.

5. Fatigue Testing - Results and Discussion

5.1. SN curves

SN curves were determined from fitting measured fatigue data points using the Basquin's law [17] which is described in Equation 2.

$$S_a = S_0 N_f^{-\frac{1}{B}} \tag{2}$$

Values of nominal stress amplitude (S_a) were obtained by dividing the applied load amplitude by the net cross section area. Statistical analysis was carried out based on the ASTM E739 [18] with a 95% confidence interval and a 50% failure probability. SN curves with confidence bands and respective data points are plotted in a double-log chart in Fig. 7.

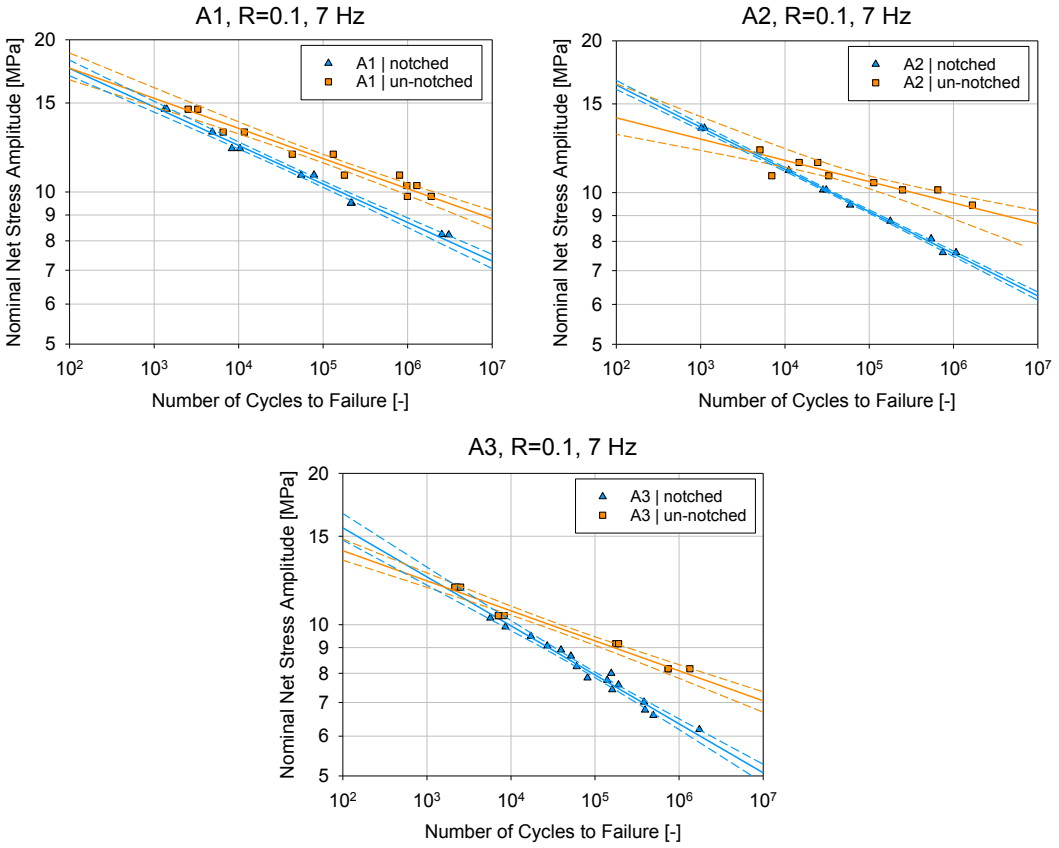

Fig. 7. SN curves of structural adhesives (notched and un-notched)

For all three adhesives a reduction of fatigue strength was observed in the presence of notches, especially at the high cycle fatigue range. Additionally, the slope of the SN curve was steeper for notched specimens, which is an important factor that represents the severity of fatigue. In the present work, this severity was defined by the fatigue strength loss (FSL):

$$FSL = 100\left(1 - 10^{-\frac{1}{B}}\right) \tag{3}$$

FSL gives the percentage of fatigue strength which is lost per decade of cycles (factor of 10 in the lifetime). Fatigue parameters of the Basquin's fitting (S_0 and B), FSL and r-squared of the linear regression of the SN curve are summarized in Table 2. As seen, linear regressions had a very good correlation with experimental data points (higher than 0.8 in all cases). Since the notch provides a preferable region for crack initiation, the values of r-squared are higher for notched tests. For all adhesives the severity of fatigue (FSL) is higher for notched samples. With regards to material properties, higher values of FSL where obtained for more ductile adhesives (A3 > A2 > A1).

Table 2. Fatigue parameters

Parameter	A1 (U)	A1 (N)	A2 (U)	A2 (N)	A3 (U)	A3 (N)
S_0 [MPa]	23.1	24.9	17.1	24.0	18.5	24.4
B [-]	16.8	13.1	23.7	11.9	16.7	10.3
FSL [%]	12.8	16.1	9.3	17.5	12.9	20.1
r-squared of linear regression [-]	0.95	0.99	0.82	0.99	0.96	0.97

The notch effect at low cycle (LCF) and high cycle fatigue (HCF) was distinct. This can be seen in Fig. 8, where the values of net nominal stress amplitude for the three adhesives (un-notched and notched) regarding lifetimes of $N_f = 10^3$ (LCF) and $N_f = 10^6$ (HCF) are shown. In Fig. 8a for LCF, notches had less than 6% of strength difference with regards to the un-notched samples. In some cases (A2 and A3), notched specimens had even higher fatigue strength. This could be explained based on the results of FEA and representative stress-strain curves of the material by the fact that at LCF the stresses causing failure are relatively high. For this reason, for both un-notched and notched specimens, a high amount of plastic deformation has likely occurred in the whole cross-section of the material. Hence, the effect of stress concentrations for the notched samples was mitigated [10]. On the other hand, for HCF, fatigue strength was strongly reduced after notching (Fig. 8b) with reductions ranging from 16.7 to 27.5%. In the HCF, it is likely that deformations were predominantly linear-elastic for the un-notched specimen. In the presence of a notch, as seen in Fig 6., stress concentrations occurred at the notch root. Regions with high stresses established a preferential region for crack initiation, thus, reducing fatigue strength [8].

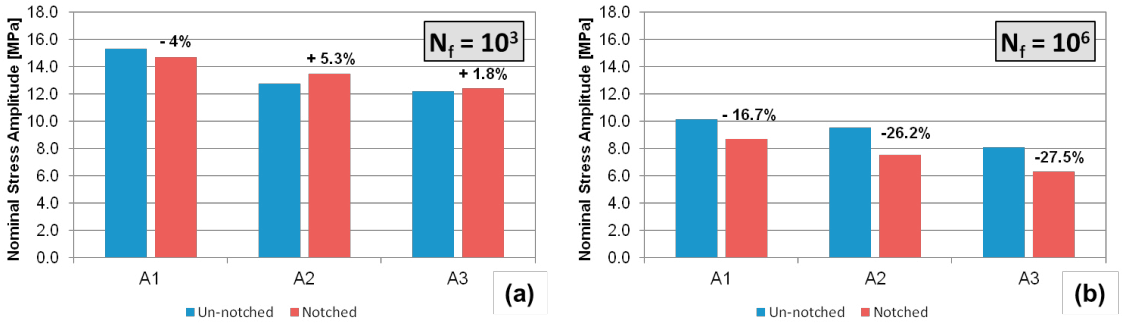

Fig. 8. Effect of notches at low and high cycle fatigue: (a) $N_f = 10^3$ and (b) $N_f = 10^6$

Adhesives had different reactions to the presence of notches. The notch sensitivity (q) of a material is defined as function of the stress concentration factor (k_T) and the fatigue notch factor (k_F), which is the ratio between un-notched and notched fatigue strength [12,19]:

$$q = \frac{k_F - 1}{k_T - 1} \tag{4}$$

Since notch sensitivity is a linear elastic property, it is more relevant to be calculated at the HCF range [20]. For this reason, q was calculated for loads related to $N_f = 10^6$. The values of q for the adhesives were: A1 = 0.10, A2 = 0.15 and A3 = 0.16. These calculations highlighted the dependence of the notch sensitivity to the material properties of the adhesives. Moreover, values of q found for the structural adhesives were significantly lower than typical values of metals [19].

In the case of metals, it is common to correlate the fatigue strength with the tensile strength under quasi-static conditions. This procedure was conducted for the adhesives under investigation and results are plotted in Fig. 9. The correlation was made for the fatigue strength of un-notched and notched samples for $N_f = 10^3$ and $N_f = 10^6$.

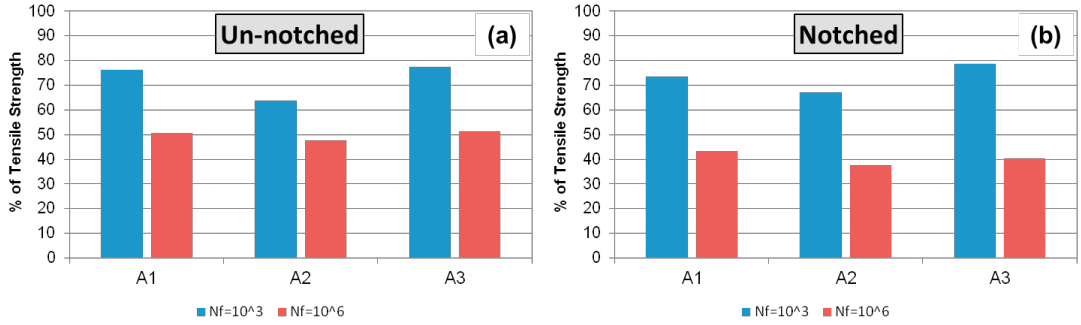

Fig. 9. Relation between fatigue strength and tensile strength: (a) un-notched specimens and (b) notched specimens

For un-notched samples (Fig. 9a) the fatigue strength was between 62 and 78% of the tensile strength for $N_f = 10^3$ and around 50% for $N_f = 10^6$. Due to the high standard deviation of the measurement of the tensile strength of the A2 adhesive 8 (see Table 1) it is possible that all adhesives would have the same percentage of the tensile strength (~75%) for $N_f = 10^3$. For the notched specimens (Fig. 9b) the same trend was observed with fatigue strength between 67 and 78% of the tensile strength for $N_f = 10^3$ and around 40% for $N_f = 10^6$.

5.2. Fractography

Fractured samples were analyzed in an optical microscope with a magnification of 30x. Fracture surfaces of all adhesives showed two distinct regions: (i) stress whitening region at highly damaged region (crack onset and slow propagation) and (ii) a region of instantaneous fracture (darker region) [3]. Orange lines were drawn in the images to define a region of 0.5 mm distance from the notch, where it is possible to observe voids and shear yielding. These are typical features on the deformation and fracture of modified epoxies [21].

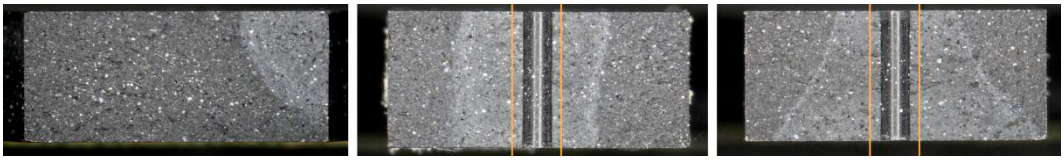

Fig. 10. Representative fracture surfaces of A1 adhesive: un-notched (left), notched-LCF (center) and notched-HCF (right)

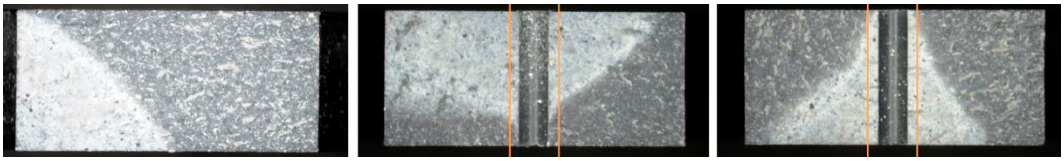

Fig. 11. Representative fracture surfaces of A2 adhesive: un-notched (left), notched-LCF (center) and notched-HCF (right)

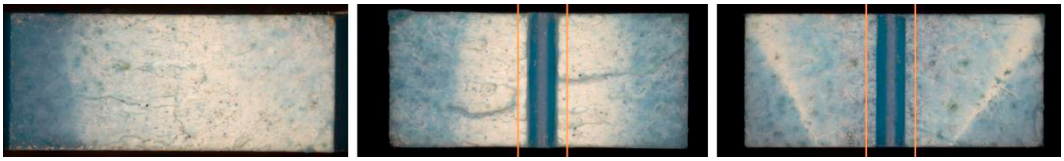

Fig. 12. Representative fracture surfaces of A3 adhesive: un-notched (left), notched-LCF (center) and notched-HCF (right)

Fractography images also revealed that the fracture surface of the most ductile adhesive (A3) is much more textured ("rough") than the surface of the other adhesives (A1 and A2) which are much more "flat", *i.e.* brittle. This behaviour occurs both for un-notched and notched specimens.

Un-notched samples showed the same fracture behavior for both LCF and HCF with crack forming at the external surface in the corners (Fig.10 to Fig.12 – left.). For notched specimens, there was a significant distinction between LCF and HCF. At LCF a great amount of plastic deformation takes place around the notch. For this reason, the whole region around the notch is highly damaged, when the crack starts the material fails completely. Therefore, the fracture surfaces (Fig.10 to Fig.12 – center) display more parallel lines on the highly stressed region. On the other hand, in the HCF (Fig.10 to Fig.12 – right), fracture surfaces evidence the formation of corner cracks [22], probably due to defects caused by drilling. Since stresses are likely predominantly elastic, the formation and propagation of cracks was slower, which caused a more triangular shape of the highly stress region.

6. Conclusions

In present work, three types of structural modified epoxy adhesives were used to investigate the effect of stress concentrations on the fatigue behavior of notched bulk specimens. SN curves of un-notched and notched specimens were determined at constant amplitude and R = 0.1 in the range between $N_f = 10^3$ (LCF) and $N_f = 10^6$ (HCF).

Based on experimental results and conducted analysis the following key conclusions can be made

- Fatigue strength was reduced due the presence of notches, especially at the HCF. Based on FEA results and stress-strain of the adhesives. This could be related to the fact that at HCF deformations were predominantly linear-elastic with stress concentrations occurring at the notch root. These highly stressed regions established a preferential region for crack initiation; hence, reducing fatigue strength at HCF. On the other hand, at LCF, the effect of stress concentration was mitigated due to plastic deformation.
- Adhesives showed different values of notch sensitivity (q) with values of q for the adhesives lower than typical value of metals.
- For un-notched samples fatigue strength was between 62 and 78% of tensile strength for $N_f = 10^3$ and around 50% for $N_f = 10^6$.
- For notched samples fatigue strength was between 67 and 78% of the tensile strength for $N_f = 10^3$ and around 40% for $N_f = 10^6$.
- Fractography evidenced the presence of voids and shear yielding around the notches. The most ductile adhesive had a much more "textured" fracture surface as compared to the other adhesives that had a more "flat" surface. Un-notched samples showed the same fracture behavior for both LCF and HCF with crack formation at the external surface. For notched samples there was a significant distinction between LCF and HCF with cracks forming at the notch root.

Acknowledgements

To the Science without Borders Program (Ciência sem Fronteiras, Vinicius Carrillo Beber 13458/13-2) and the Coordination of Improvement of Higher Education Personnel (CAPES – Brazil).

References

[1] M. Abdel Wahab, Fatigue in Adhesively Bonded Joints: A Review, ISRN Mat Sci 2012 (3) (2012) 1–25.
[2] H. Khoramishad, A.D. Crocombe, K.B. Katnam, I.A. Ashcroft, Predicting fatigue damage in adhesively bonded joints using a cohesive zone model, Int J Fatigue 32 (7) (2010) 1146–1158.
[3] K.B. Katnam, A.J. Comer, W.F. Stanley, M. Buggy, T.M. Young, Investigating tensile behaviour of toughened epoxy paste adhesives using circumferentially notched cylindrical bulk specimens, Int J Adhes Adhes 37 (2012) 3–10.
[4] L.F.M. da Silva, A. Öchsner, R.D. Adams, Handbook of adhesion technology, Springer, Berlin, 2011.
[5] H. Neuber, Theory of notch stresses: Principles for exact calculation of strength with reference to structural

form and material, Springer, Berlin, 1958.
[6] R.E. Peterson, Notch sensitivity, Metal fatigue (1959) 293–306.
[7] M. Takano, L.E. Nielsen, The notch sensitivity of polymeric materials, J Appl Polym Sci 20 (8) (1976) 2193–2207.
[8] M.C. Sobieraj, J.E. Murphy, J.G. Brinkman, S.M. Kurtz, C.M. Rimnac, Notched fatigue behavior of PEEK, Biomaterials 31 (35) (2010) 9156–9162.
[9] L. Susmel, D. Taylor, A novel formulation of the theory of critical distances to estimate lifetime of notched components in the medium-cycle fatigue regime, Fat Frac Eng Mat Struct 30 (7) (2007) 567–581.
[10] Y. Zhou, P.K. Mallick, Fatigue performance of an injection-molded short E-glass fiber-reinforced polyamide 6,6. I. Effects of orientation, holes, and weld line, Polym. Compos. 27 (2) (2006) 230–237.
[11] D. Hoey, D. Taylor, Fatigue in porous PMMA: The effect of stress concentrations, Int J Fatigue 30 (6) (2008) 989–995.
[12] S. Mortazavian, A. Fatemi, Notch Effects on Fatigue Behavior of Thermoplastics, AMR 891-892 (2014) 1403–1409.
[13] V.C. Beber, P.H.E. Fernandes, B. Schneider, M. Brede, Effect of notch size on the fatigue damage behaviour of toughened epoxy adhesive specimens, J Adhesion 93 (1-2) (2017) 113–126.
[14] M.C. Sobieraj, S.M. Kurtz, C.M. Rimnac, Notch strengthening and hardening behavior of conventional and highly crosslinked UHMWPE under applied tensile loading, Biomaterials 26 (17) (2005) 3411–3426.
[15] N. Burst, D.O. Adams, H.E. Gascoigne, Investigating the Thin-Film Versus Bulk Material Properties of Structural Adhesives, J Adhesion 87 (1) (2011) 72–92.
[16] D. Morin, G. Haugou, B. Bennani, F. Lauro, Identification of a new failure criterion for toughened epoxy adhesive, Eng Fract Mech 77 (17) (2010) 3481–3500.
[17] O. Basquin, The exponential law of endurance tests, Proc. Am. Soc. Test. Mat. 10 (1910) 625–630.
[18] E08 Committee, Practice for Statistical Analysis of Linear or Linearized Stress-Life (S-N) and Strain-Life (-N) Fatigue Data, ASTM International, West Conshohocken, PA, 2015.
[19] M. Benedetti, V. Fontanari, M. Allahkarami, J.C. Hanan, M. Bandini, On the combination of the critical distance theory with a multiaxial fatigue criterion for predicting the fatigue strength of notched and plain shot-peened parts, Int J Fatigue 93 (2016) 133–147.
[20] R.W. Hertzberg, R.P. Vinci, J.L. Hertzberg, Deformation and fracture mechanics of engineering materials, 5th ed., John Wiley & Sons, Hoboken, N.J., Chichester, 2013.
[21] A.J. Kinloch, S.J. Shaw, D. Tod, D. Hunston, Deformation and fracture behaviour of a rubber-toughened epoxy: Part 1 - Microstructure and fracture studies, Polymer 24 (1983) 1341-1354.
[22] H.A. Richard, M. Sander, Ermüdungsrisse: Erkennen, sicher beurteilen, vermeiden, 3rd ed., Springer Vieweg, Wiesbaden, 2012.